

# Weak Interactions in Top-Quark Pair Production at Hadron Colliders: An Update

J.H. Kühn <sup>a</sup>, A. Scharf <sup>b</sup> and P. Uwer <sup>c</sup>

<sup>a</sup>*Institut für Theoretische Teilchenphysik, Karlsruhe Institut of Technology (KIT)*

*76128 Karlsruhe, Germany*

<sup>b</sup>*Institut für Theoretische Physik und Astrophysik, Universität Würzburg*

*D-97074 Würzburg, Germany*

<sup>c</sup>*Institut für Physik, Humboldt-Universität zu Berlin*

*12489 Berlin, Germany*

Weak corrections for top-quark pair production at hadron colliders are revisited. Predictions for collider energies of 8 TeV, adopted to the present LHC run, and for 14 TeV, presumably relevant for the next round of LHC experiments, are presented. Kinematic regions with large momentum transfer are identified, where the corrections become large and may lead to strong distortions of differential distributions, thus mimicking anomalous top quark couplings. As a complementary case we investigate the threshold region, corresponding to configurations with small relative velocity between top and antitop quark, which is particularly sensitive to the top-quark Yukawa coupling. We demonstrate, that nontrivial upper limits on this coupling are well within reach of ongoing experiments.

# 1 Introduction

During the past years the determination of the top quark mass, its couplings, production and decay rates has been pursued successfully at the Tevatron. Based on an integrated luminosity of more than  $5 \text{ fb}^{-1}$  per experiment collected by both CDF and D0 at 1.96 TeV, a sample of nearly 100000 top quark pairs has been produced. The analysis of these events has lead, for example, to a top mass determination of  $M_t = 173.18 \pm 0.94 \text{ GeV}$  [1], corresponding to a relative error of about half percent. The total production cross section  $\sigma_{t\bar{t}} = 7.65 \pm 0.42 \text{ pb}$  [2] determined at Tevatron is in very good agreement with the theory predictions [3–14]. The same is true for the cross section measurements performed at the LHC. Very recently also the  $t\bar{t}$  invariant mass distribution has been measured at LHC over a wide kinematical range [15, 16]. Similar to the cross section measurements the results are in agreement with the Standard Model (SM) predictions. In contrast, surprising deviations from the theory predictions have been observed in the Tevatron experiments [17–20] by investigating the so-called charge asymmetry predicted originally fifteen years ago [21, 22]. (For recent discussions of theoretical predictions in the context of the SM see for example Refs. [23–27]).

Although these are impressive achievements already now, expectations for top quark physics at the LHC fly even higher. Based on integrated luminosities close to  $5 \text{ fb}^{-1}$  per experiment at 7 TeV, the top mass has been determined in a combined analysis to  $M_t = 173.3 \pm 1.4 \text{ GeV}$  [28] already now. With an integrated luminosity of more than  $20 \text{ fb}^{-1}$  per experiment collected recently at 8 TeV, several million top-quark pairs per experiment have been produced. The high energy run at 14 TeV with its expected integrated luminosity of  $100 \text{ fb}^{-1}$ , will deliver about  $10^8$  top quark pairs per experiment during the coming years. The LHC is, obviously, a factory of top quarks, allowing for a precise determination of their properties and their production dynamics in a large kinematic region. The large center of mass energy available at the LHC will thus be used to investigate top production with partonic subenergies of several TeV and thus explore the point-like nature of the heaviest of the fundamental particles. On the theoretical side precise predictions valid at highest accessible energies are required. With the recently completed next-to-next-to leading order QCD predictions [7–10] a major step has been taken. However when it comes to ultimate precision or highest energies weak corrections significantly affect predictions within the Standard Model. Two kinematic regions are of particular interest:

- i.*) Hard scattering events with partonic subenergies  $\hat{s}$  and momentum transfers  $|\hat{t}|$  and  $|\hat{u}|$  ( $\hat{s}, \hat{u}$  and  $\hat{t}$  denote the partonic Mandelstam variables) far larger than  $M_t$  are affected by large negative corrections. These may reach nearly twenty percent, affecting transverse-momentum and angular distributions, and might well mimic anomalous top quark couplings. These negative corrections—if not taken into account in the theoretical predictions—could also hide a possible rise of the cross section due to a heavy resonance.
- ii.*) The rate for events very close to the production threshold, with relative top-antitop velocity  $\beta \leq M_H/M_t$  is enhanced by the exchange of the relatively light Higgs boson.

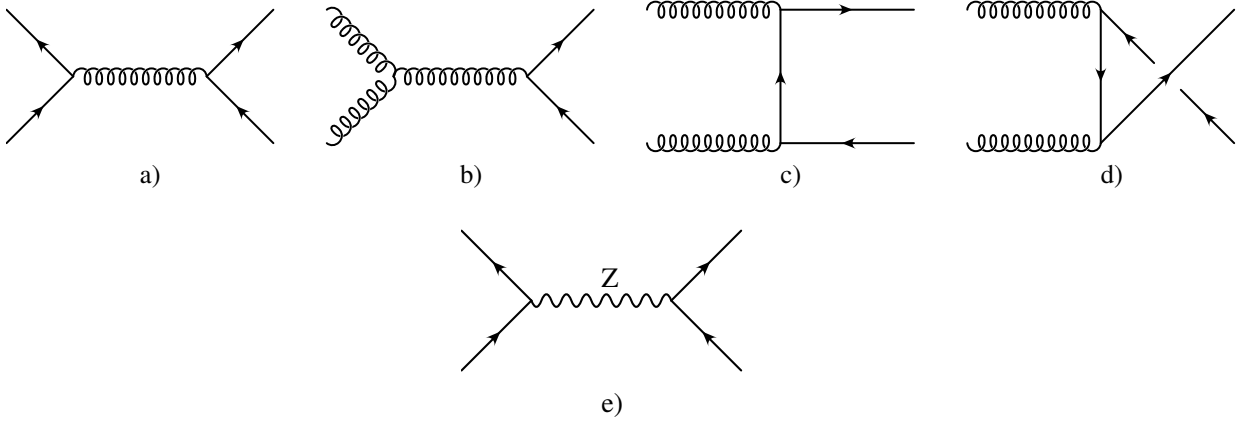


Figure 1: Lowest order QCD (a–d) and weak (e) amplitudes

This effect can be approximately described by a Yukawa potential and is reminiscent of Sommerfeld rescattering corrections.

Weak corrections to top quark pair production have first been studied twenty years ago [29]. The complete results, where some deficiencies were corrected and the result given in closed analytical form, can be found in Refs. [30, 31] and Refs. [32, 33] for quark- and gluon-induced processes, respectively. Numerical results (which, however, differed from those presented in Refs. [32, 33] and were corrected later) have been published in Ref. [34]. Purely electromagnetic corrections, which can be handled separately from the weak corrections, are evaluated in Ref. [35]. As a consequence of cancellations between the positive contributions from  $\gamma g$ -fusion and negative corrections to  $q\bar{q}$ -annihilation the combined effect amounts at most to  $-4\%$ , if one considers  $p_T$ -values as high as 1.5 TeV. The impact on the  $\sqrt{\hat{s}}$  distribution remains below 1%. The details of these corrections are strongly cut-dependent and we refer to Ref. [35] for details.

In the present paper we refrain from repeating the somewhat lengthy analytical formulae for the weak corrections and concentrate on the physics implications. In particular we also update results previously obtained using modern parton distribution functions (PDF's) and the most recent values for the input parameters.

## 2 Large momentum transfers

Before entering the detailed numerical discussion, let us recall the basic qualitative aspects of weak corrections for the present case. With the Born amplitudes being of order  $\alpha_s$  (Figs. 1 a)-d) both for quark and gluon induced QCD processes, and of order  $\alpha_{\text{weak}}$  for the lowest order weak process (Fig. 1 e), weak corrections start entering the cross section at loop-induced order  $\alpha_s^2 \alpha_{\text{weak}}$  only. The absence of an interference term between the lowest order strong and

neutral current amplitudes in the quark induced process, which would be of order  $\alpha_s\alpha_{\text{weak}}$ , follows trivially from the different colour flow in the two relevant amplitudes Fig. 1a and e, respectively.

Sample diagrams for weak corrections to quark- and gluon-induced amplitudes are shown in Figs. 2 and 3. For gluon fusion weak effects start as corrections to the QCD induced amplitudes.

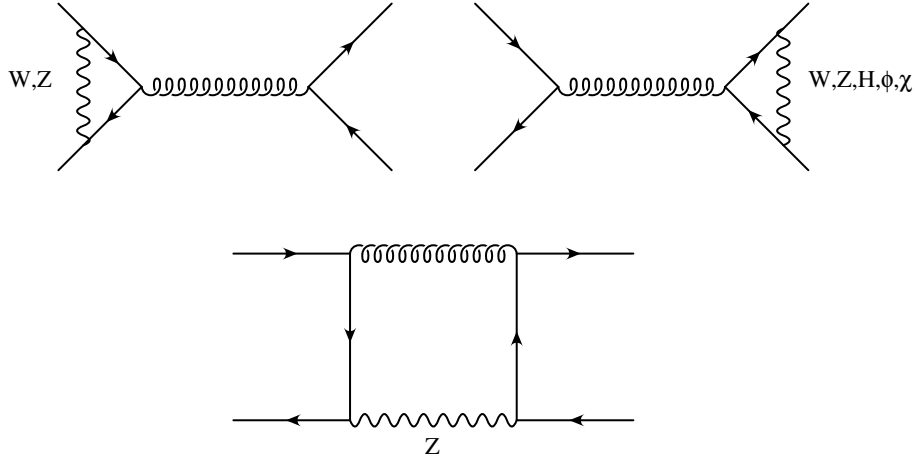


Figure 2: Sample diagrams for the virtual corrections.

For quark-antiquark annihilation the situation is more involved in view of a specific class of order  $\alpha_s^2\alpha_{\text{weak}}$  contributions to the quark induced processes, which must be considered separately. In this case weak and strong interaction are intimately intertwined, and corrections with virtual and real (Fig. 4) gluon emission must be combined to arrive at an infrared finite result. The proper combination of real and virtual contributions is illustrated in Fig. 5. This issue is discussed in more detail in Ref. [30]. Only a specific combination of couplings is present in this case: The top quark triangle in Fig. 5 is attached to two gluons with vector coupling. As long as we are interested in parity-even observables (like cross section or  $p_T$ -distributions), the light quark coupling to the  $Z$  boson is therefore restricted to its axial coupling  $g_A^q$  proportional to its isospin  $I_3^q$ . This, in turn, leads to a strong cancellation of this specific type of correction between u- and d-quark induced processes. Since, furthermore, these contributions are small (see Fig IV.3 of Ref. [30]) for one species of quarks already, (less than one percent at threshold and about two percent at very high energies), this group of corrections could be neglected in the following discussion. This observation might, eventually, facilitate the combination of strong and weak corrections discussed at the end of this paper.

For large parton energies the total corrections are negative, for quark- as well as for gluon-induced processes. However, as a consequence of the non-vanishing weak charge both in the initial as well as in the final state, the corrections for quark induced top production are about twice those of the gluon induced process, with important consequences for the energy dependence of the corrections.

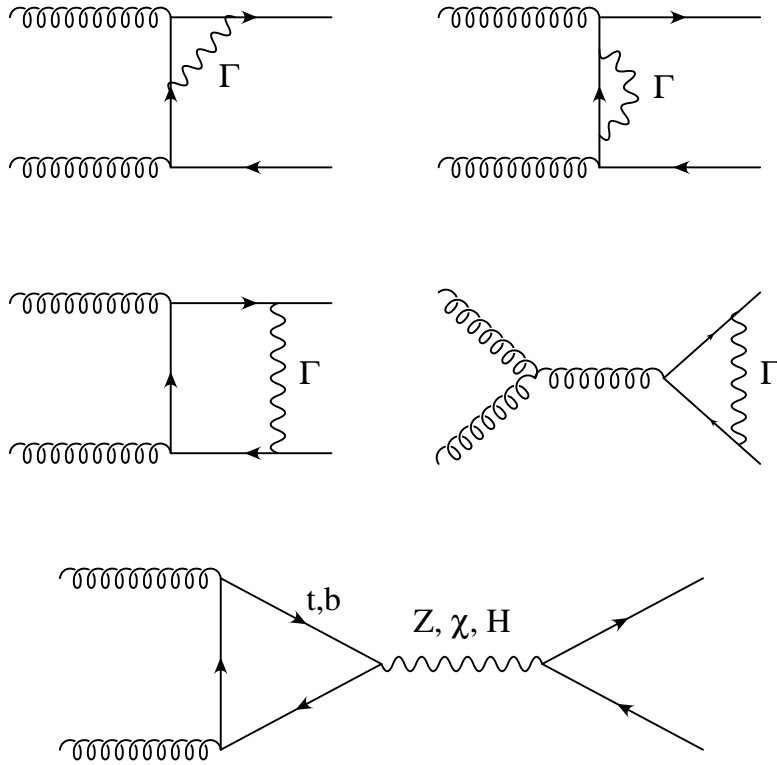


Figure 3: Sample diagrams for the virtual corrections.  $\Gamma$  stands for all contributions from gauge boson, Goldstone boson and Higgs exchange.

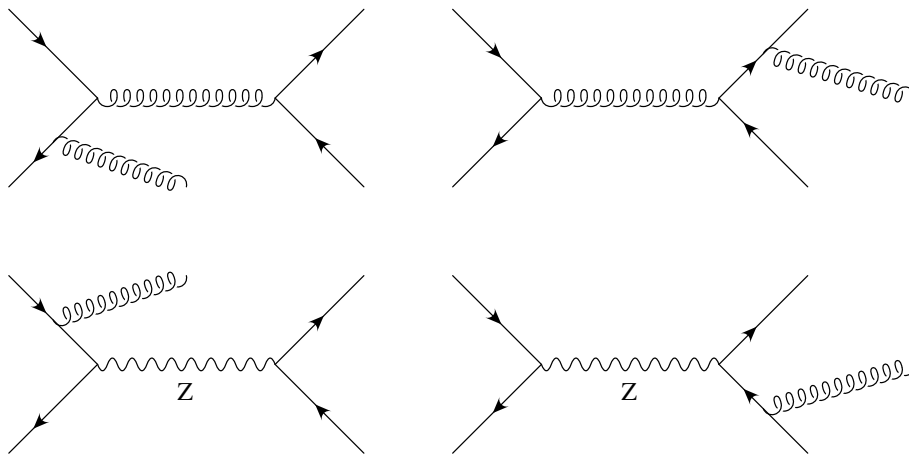


Figure 4: Sample diagrams for the real corrections to the quark-induced process.

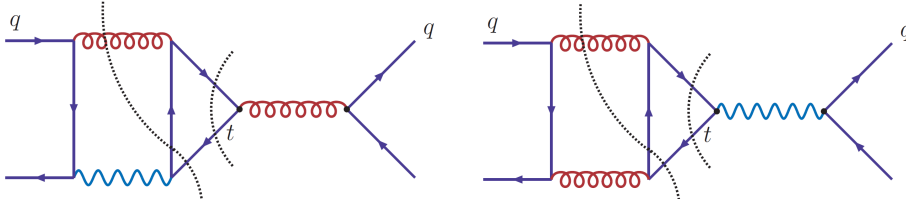


Figure 5: Sample diagrams for the proper combination of virtual and real corrections to the quark-induced process.

As discussed in Ref. [33] for proton-proton collisions at 14 TeV, (denoted by LHC14 in the following), the total cross section for top production is dominated by gluon fusion. In contrast, production of top quarks with large invariant mass of the  $t\bar{t}$ -system or at large transverse momenta is mainly induced by quark-antiquark annihilation, a consequence of the different parton luminosities (see Fig. 6 for LHC operating at 14 TeV and Fig. 7 for LHC running at 8 TeV). The relative increase of the the quark-induced processes in combination with the different strength of the weak corrections for the two reactions thus leads to an additional increase of weak corrections for very large transverse momenta.

For the numerical results presented in this paper we use the parton distribution function MSTW2008NNLO PDF set<sup>1</sup> [36], evaluated at a factorization scale  $\mu_F = M_t$ , and the coupling constants

$$\alpha(2M_t) = \frac{1}{126.3}, \quad \alpha_s = 0.1, \quad \sin^2 \theta_W = 0.231.$$

For the masses we use

$$M_Z = 91.1876 \text{ GeV}, \quad M_W = 80.425 \text{ GeV}, \quad M_b = 4.82 \text{ GeV}, \quad M_t = 173.2 \text{ GeV},$$

and, if not stated otherwise,  $M_H = 126 \text{ GeV}$ . The weak mixing angle and the masses of W- and Z-boson are, of course, interdependent. Nevertheless, we expect that, using the  $\overline{\text{MS}}$  value for the weak mixing angle, some of the (uncalculated) higher-order corrections are included and, therefore, a better phenomenological description is achieved. For the details of the renormalisation we refer to Ref. [33].

Another important aspect is the nontrivial angular dependence of the weak corrections. As is well known, the leading Sudakov logarithms proportional  $\log^2(s/M_W^2)$  are only dependent on the (weak) charge of the incoming and outgoing particles, subleading terms may exhibit a nontrivial angular dependence (see e.g. [38, 39]). This is reflected in characteristic angular dependent virtual corrections which affect the rapidity distributions of top quarks at the LHC and might well mimic anomalous couplings of the particles involved.

Let us now enter the description of the corrections in more detail. The corrections at the partonic level are shown in Fig. 8 for quark and gluon induced processes as functions of  $\hat{s}$ . For

<sup>1</sup>We follow closely the setup used for the NNLO QCD corrections so that the results presented here can be combined with the QCD corrections.

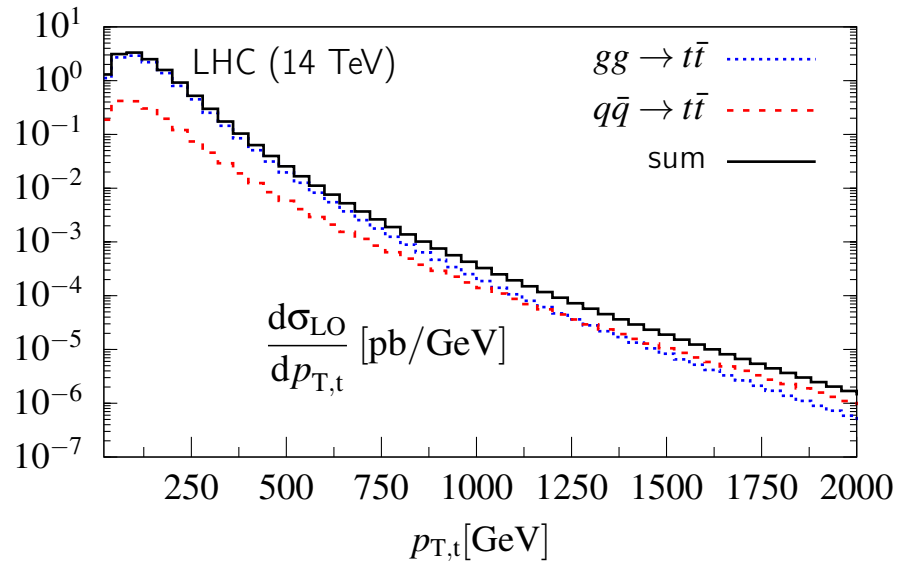
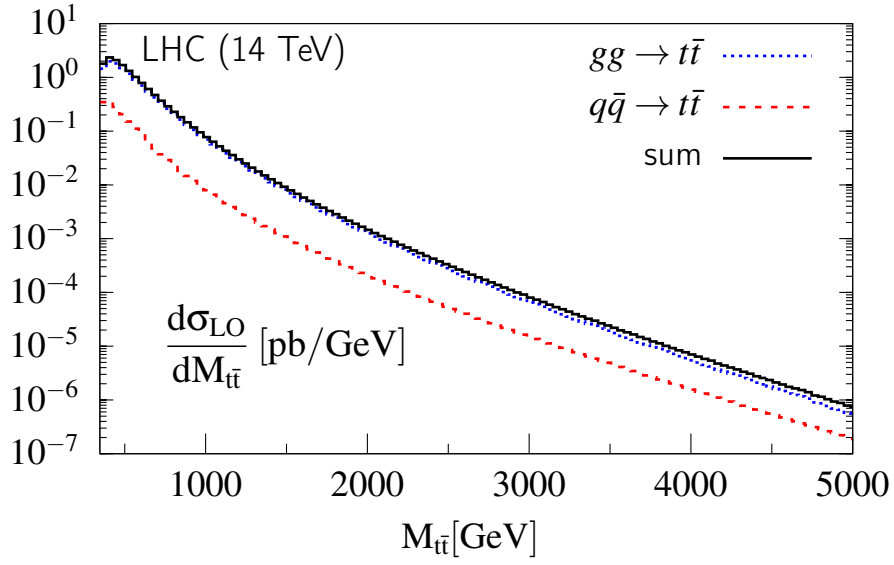


Figure 6: Leading-order differential cross section for the LHC (14 TeV) as a function of  $p_T$  and  $M_{t\bar{t}}$ . Shown is the sum (full) and the contributions from gluon fusion (dashed) and quark–antiquark annihilation (dotted).

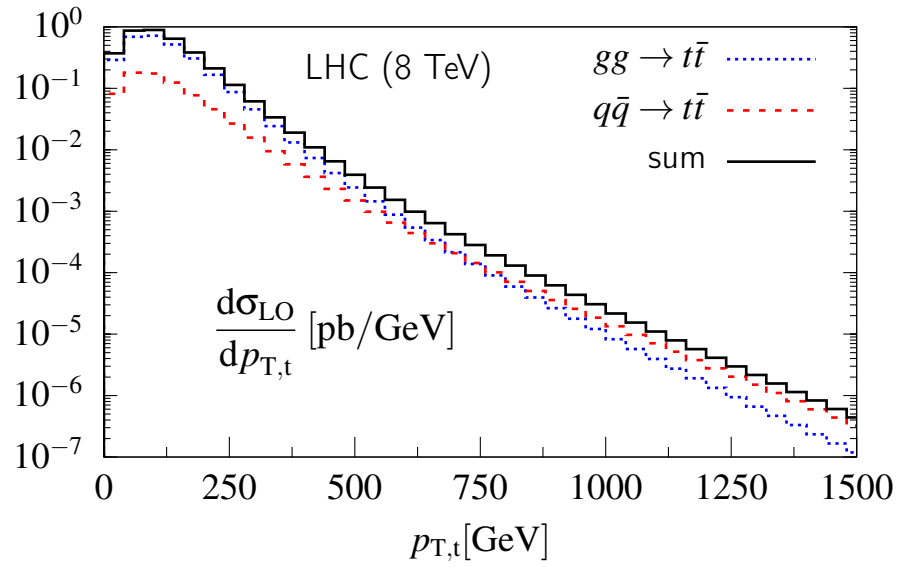
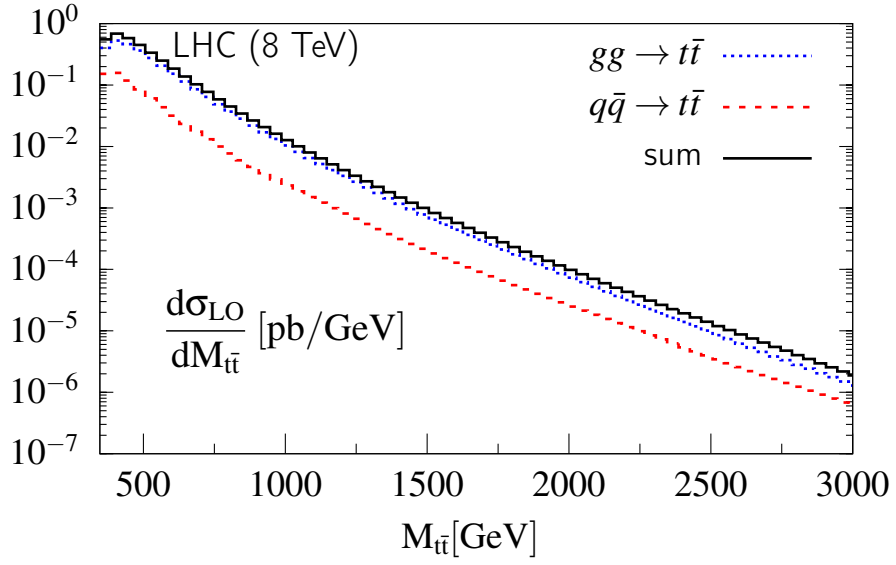


Figure 7: Leading-order differential cross section for the LHC (8TeV) as a function of  $p_T$  and  $M_{t\bar{t}}$ . Shown is the sum (full) and the contributions from gluon fusion (dashed) and quark–antiquark annihilation (dotted).

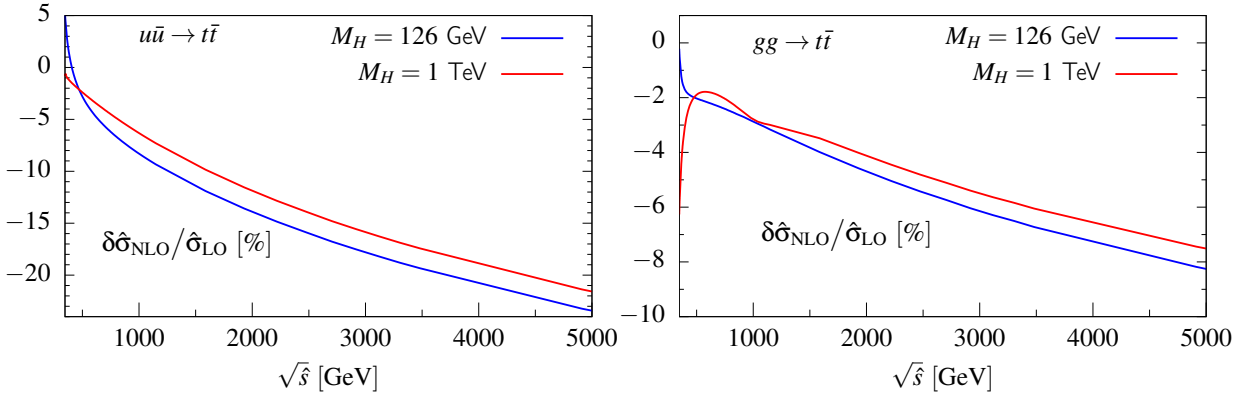


Figure 8: Relative weak corrections at parton level for the quark- and gluon-induced reactions as functions of the squared parton energy  $\hat{s}$  for two characteristic masses of the Higgs boson.

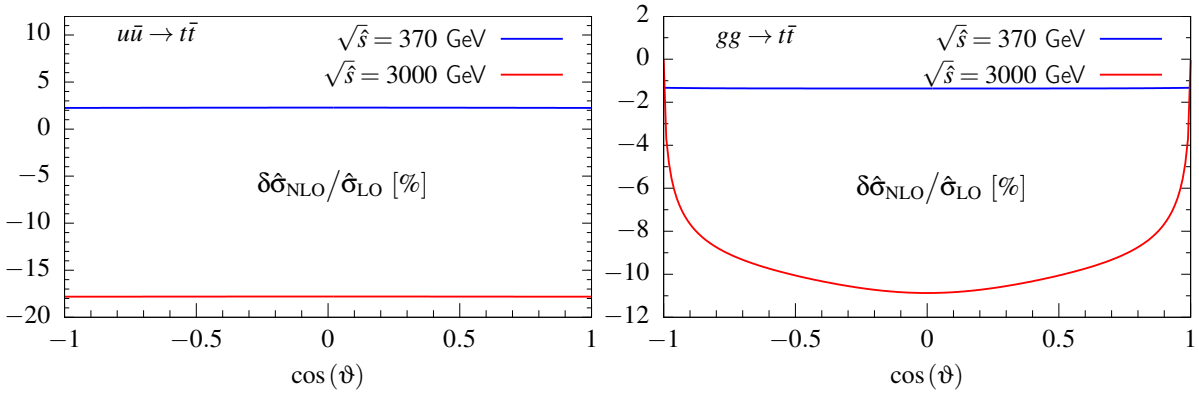


Figure 9: Relative weak corrections for the quark- and gluon-induced reactions as functions of the scattering angle close to threshold ( $\sqrt{\hat{s}} = 370 \text{ GeV}$ ) and at high energies ( $\sqrt{\hat{s}} = 3 \text{ TeV}$ )

the quark–anti-quark channel we include only the infrared finite vertex corrections which are responsible for the Sudakov suppression at large momentum transfer. The box contributions for the  $q\bar{q}$  process are important only for the charge-asymmetric piece [23–27], and can be neglected in the present context. As expected, away from very small  $\hat{s}$  the corrections are negative and about twice as large for quark- compared to gluon-induced processes. Only very close to threshold one observes corrections which become positive for a light Higgs boson and will be discussed in section 3. For the fictitious case of  $M_H = 1$  TeV two pronounced structures are visible in the gluon-fusion channel: The interference between the Born amplitude and the  $s$ -channel Higgs boson contribution (last diagram of Fig.3) is visible as slight depletion around 1 TeV, the interference with the  $Z$  plus  $\chi_Z$  contribution arising from the same diagram is responsible for the dip close to threshold. For  $M_H = 126$  GeV this dip is overcompensated by the positive contribution of roughly 5% from the Yukawa interaction discussed in more detail in section 3. This same difference of 5% between  $M_H = 126$  GeV and 1 TeV is also visible in the threshold behaviour of the  $q\bar{q}$ -initiated reaction.

The angular dependence of the corrections is shown in Fig. 9 separately for quark and gluon induced processes close to threshold at 370 GeV (upper blue curve) and for 3 TeV (lower red line). Let us, in a first step, discuss the results for the quark-induced reaction (Fig. 9 left). Again we restrict the analysis to the vertex correction. Close to threshold the process is dominated by (isotropic)  $S$ -waves, at high energies (3 TeV) the Dirac form factor dominates both for Born amplitude and correction. This leads to a constant ratio as function of the scattering angle. At low energies ( $\sqrt{\hat{s}} = 370$  GeV) we find a positive correction of about 2%. At large energies the Sudakov suppression leads to negative corrections of about  $-18\%$ . Note that the box diagrams while not particularly enhanced would lead to sizable asymmetric and small symmetric corrections. For details we refer to Ref. [25]. The gluon induced part, in contrast, is markedly angular dependent. For large  $\hat{s}$  and small scattering angle the corrections are small, since the Sudakov-like behaviour cannot be expected in this case. At ninety degrees, in contrast, the Sudakov limit is applicable and the corrections become large.

Let us now discuss observables at the hadron level. In difference to the discussion at parton level we include in the analysis now also box-contributions and real corrections, thus the full set of corrections are investigated. The corrections for the total cross section are shown in Fig. 10 as function of  $\sqrt{s}$ , for two characteristic choices of the Higgs mass,  $M_H = 126$  GeV and 1000 GeV. We allow  $M_H$  to move away from its recently determined value [40,41] to illustrate the effect of the Higgs-top Yukawa coupling. The corrections are evidently small, of order minus two percent for all LHC energies and only moderately sensitive to  $M_H$ . In addition we demonstrate the impact of an enhanced Yukawa coupling with  $g_Y = 2g_Y^{SM}$  discussed in more detail in section 3. In this case the negative corrections from the large transverse momentum region are overcompensated by the positive ones for small  $t\bar{t}$  masses. Given the recent progress concerning the NNLO QCD calculations the theoretical uncertainties will eventually reach 3–4%. At this level of accuracy the weak corrections become important and need to be taken into account. As reference we show in Fig. 11 the relative weak correction as function of the top-quark mass. At 8 TeV centre of mass energy the corrections are about  $-1.7\%$ . At 14 TeV the high-energy regime of the cross section becomes more accessible leading to slightly

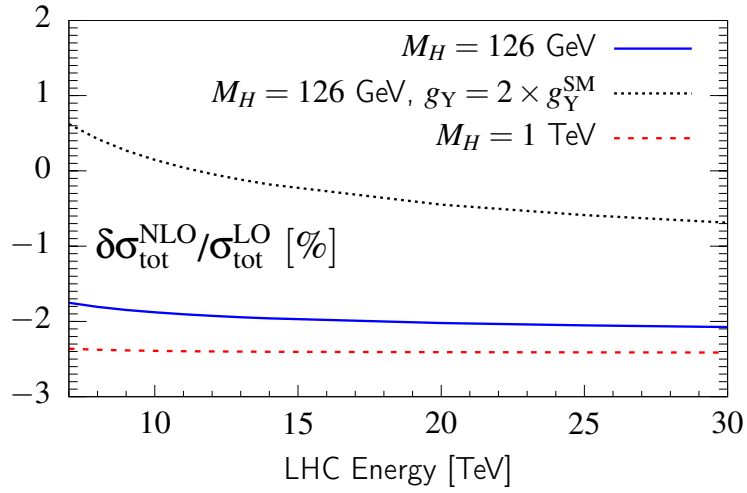


Figure 10: Relative weak corrections for the total cross section functions of the total cms energy for three different masses of the Higgs boson.

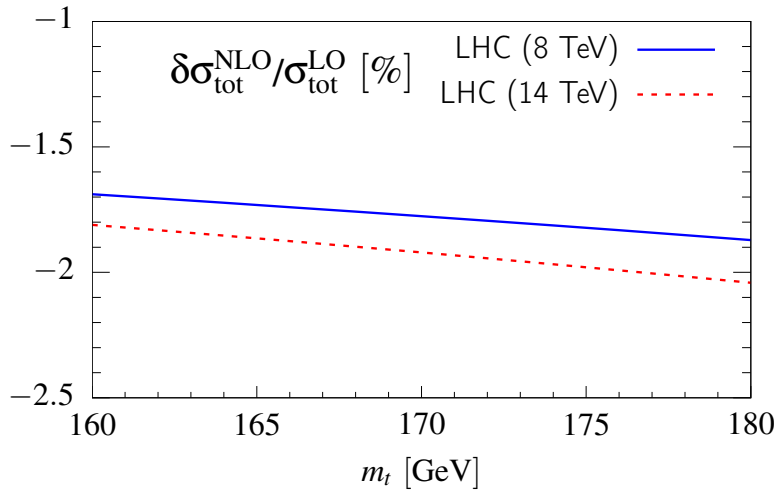


Figure 11: Relative corrections as function of the top-quark mass.

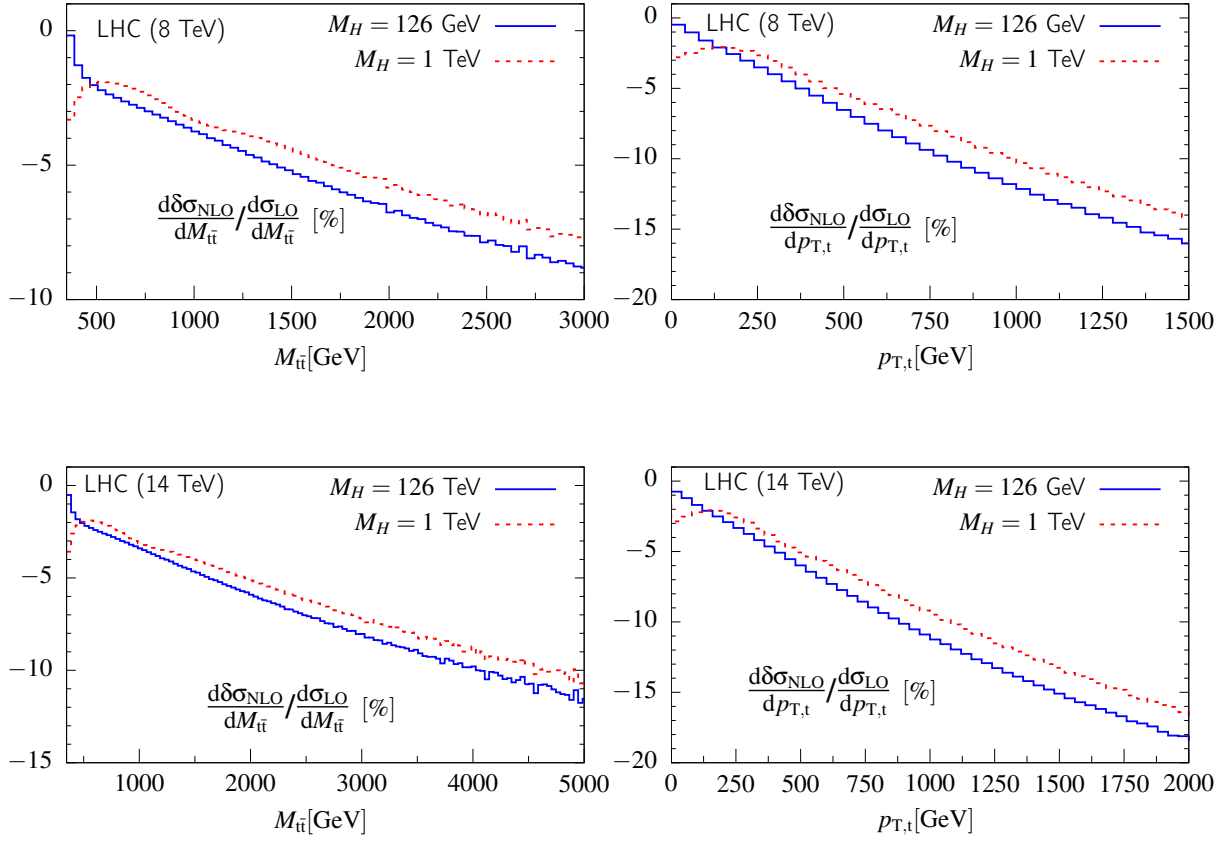


Figure 12: Relative weak corrections for the invariant  $t\bar{t}$  mass (left) and transverse momentum (right) distribution for LHC8 (upper) and LHC14 (lower plots) and for Higgs masses of 126 GeV and 1 TeV.

larger corrections of order of  $-1.9\%$ . The situation is drastically different, once we consider differential distributions in the region of large transverse momenta  $p_T$  or large masses  $M_{t\bar{t}}$  of the  $t\bar{t}$  system. The corrections are shown in Fig. 12 for proton-proton collisions with center of mass energies of 8 TeV and 14 TeV both for the  $p_T$ - and the  $M_{t\bar{t}}$ -distributions. For illustration we again present the relative corrections for Higgs masses of 126 GeV and 1 TeV. The strong increase with increasing  $p_T$  is evident. Based on the present data sample, corresponding to more than  $20 \text{ fb}^{-1}$ , corrections close to  $-10\%$  could be observed at 8 TeV.

To investigate the angular dependence of the  $t\bar{t}$  system in its center of mass frame one could consider the distribution in the rapidity difference  $\Delta y_{t\bar{t}} = y_t - y_{\bar{t}}$  which, for fixed  $M_{t\bar{t}}$  can be directly translated into the angular distribution. To illustrate the distributions and the size of the corrections, the differential distributions  $d\sigma/d\Delta y_{t\bar{t}}$  are shown in Fig.13 for 8 (left) and 14 TeV (right), considering only events with  $M_{t\bar{t}}$  larger than 1 TeV in the former and 2 TeV in the latter case. The corresponding corrections are also displayed in Fig.13. The pronounced peaking of

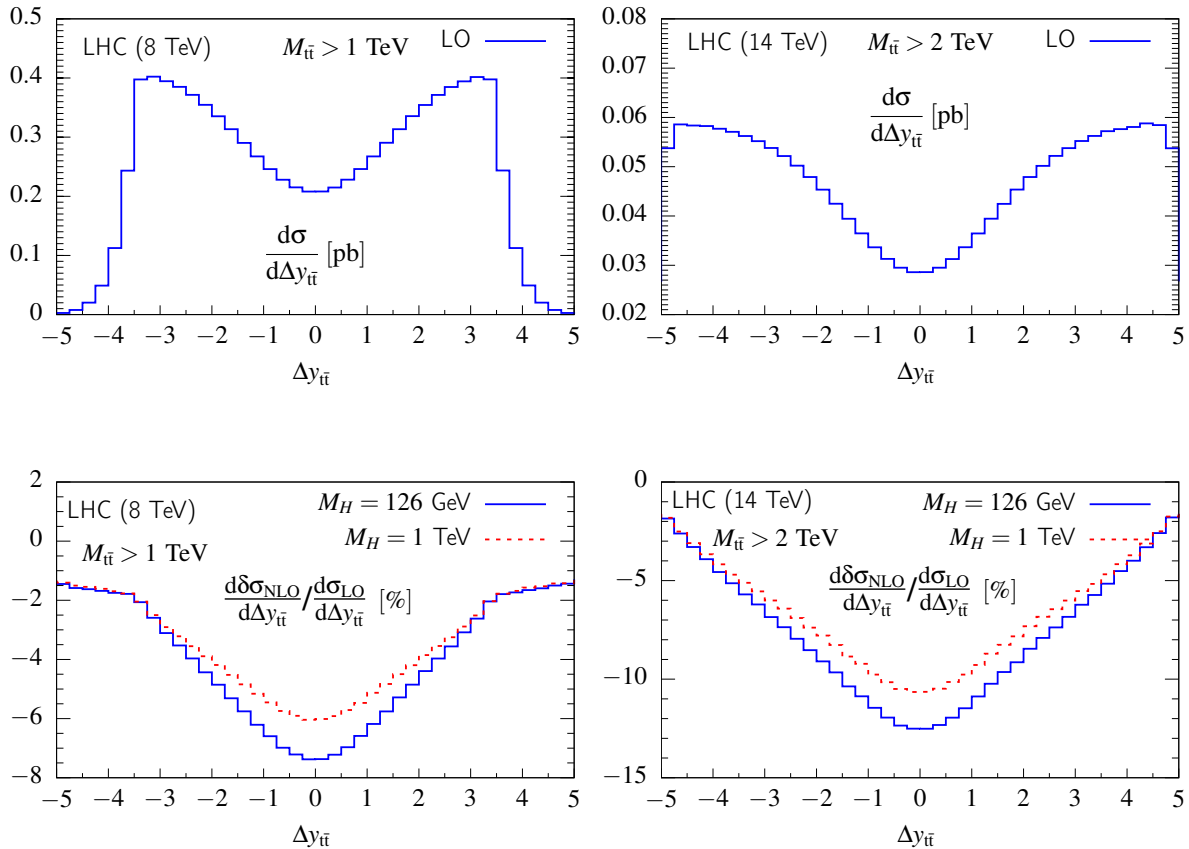


Figure 13: Rapidity distributions with invariant mass cuts at leading order (upper plots) and relative weak corrections to these distributions (lower plots) for LHC8 (left) and LHC14 (right).

the cross section for large rapidity differences in Fig.13 (top) is an obvious consequence of the  $t$ -channel singularity, the enhanced negative corrections around  $\Delta y_{i\bar{i}} = 0$  in Fig.13 (bottom) are a consequence of the Sudakov condition  $\hat{s}$  and  $|\hat{t}| \gg M_W^2$ . Since the distribution in  $\Delta y_{i\bar{i}}$  is at the same time sensitive to anomalous couplings, these could well be masked by the large radiative corrections.

Let us at this point speculate about the combination of weak and QCD corrections. Clearly, the evaluation of corrections of  $O(\alpha_s\alpha)$  is out of reach in the foreseeable future. Thus, strictly speaking, both a multiplicative (of the form  $(1 + \delta_{QCD})(1 + \delta_W)$ ) and an additive (of the form  $(1 + \delta_{QCD} + \delta_W)$ ) treatment is equally justified. The difference between the two assumptions can be considered as an estimate of the theory uncertainty. It may be useful to devise a strategy, how to implement eventually the major part of the combined corrections. As mentioned in the beginning, QED and purely weak corrections can be treated separately in the present case. Furthermore, QED corrections are small and the resulting uncertainty of combined QCD and

QED terms even smaller. In principle, by adjusting color coefficients, the recently available two-loop QCD corrections could be employed to arrive at the full combined QED and QCD results. Concerning the weak corrections, we observe that a major part of the QCD corrections originates from configurations involving soft and/or collinear emission. Let us then reconstruct the effective two-body kinematics by using the  $t\bar{t}$  invariant mass as  $\hat{s}$  and the scattering angle with respect to the beam direction, as defined in the  $t\bar{t}$  rest frame as partonic scattering angle. Using this information would allow to apply the weak correction factor which also depends on  $\hat{s}$  and  $\hat{t}$  only. It remains to be seen, to which extent this approach can be implemented in currently available event generators.

### 3 The top-pair threshold region and the Yukawa coupling

As illustrated in Fig. 8, the corrections for top-pair production very close to threshold exhibit a significant dependence on the mass of the Higgs boson. In fact, both for quark and gluon induced process the difference in the correction between a light ( $M_H = 126$  GeV) and a heavy ( $M_H = 1000$  GeV) Higgs boson amounts to about 5%. This effect has been discussed in some detail for pair production at an electron-positron collider [43–47] and for quark-antiquark collisions [47] and is closely related to the well-known Sommerfeld rescattering corrections, originally obtained in the framework of QED. Similar considerations are also applicable to gluon fusion [33].

For a Yukawa potential induced by the Higgs exchange,

$$V_Y(r) = -\kappa \frac{1}{r} e^{-r/r_Y} \text{ with } \kappa = \frac{g_Y^2}{4\pi} = \frac{\sqrt{2}G_F M_t^2}{4\pi} \approx 0.0337 \text{ and } r_Y = 1/M_H, \quad (1)$$

the dominant correction evaluated directly at threshold is given by the factor  $1 + \kappa \frac{M_t}{M_H}$ . (The full result can be found in [43, 46].) Indeed the difference of 5% between the heavy and the light Higgs boson is well consistent with this simple approximation. For quark-antiquark annihilation the positive offset is shown in Fig.8 (left). For gluon fusion the Yukawa enhancement is partially masked by a negative contribution originating from the interference of the tree-level amplitude with the amplitude from the triangle diagrams with  $Z$  and  $\chi_Z$  in the  $s$ -channel (Fig. 3). The difference, however, between a heavy and a light Higgs boson of about 5% remains unchanged.

As evident from Fig.8, the Yukawa enhancement is located in the region close to threshold, with relative  $t\bar{t}$ -velocity  $\beta$  less than  $M_H/M_t$ . For the moment we consider the weak corrections as an overall  $\beta$ -dependent factor which multiplies the complicated threshold behaviour induced by the partly attractive, partly repulsive QCD potential. (For QCD effects see e.g. [42] and references therein.) In principle the effect of a light Higgs exchange could be split into a short range piece, which leads to a  $\beta$ -independent correction term, and a long-range piece, which can be absorbed by adding Yukawa and QCD potential. The energy dependence can then be obtained from a Green's function treatment. This approach has been discussed in more

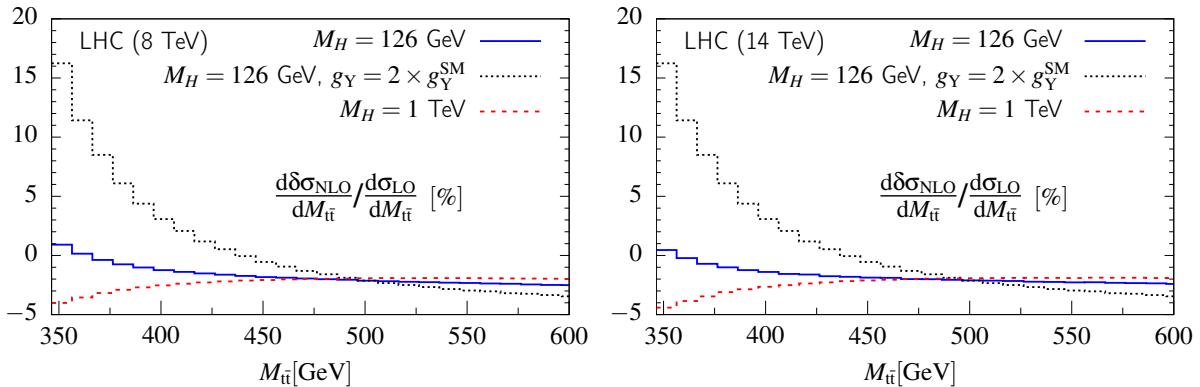


Figure 14: Relative weak corrections for the mass distribution in the framework of the SM assuming  $M_H = 126$  GeV (solid blue curve) and 1000 GeV (dashed red curve), and for the case of an enhanced Yukawa coupling  $g_Y = 2g_Y^{SM}$  with  $M_H = 126$  GeV (dotted black curve). The two plots represent LHC8 and LHC14.

detail in [47] for the cases of top production in electron-positron and quark-antiquark annihilation. Since  $r_Y$ , the characteristic length of the Yukawa potential, is still significantly smaller than  $r_B$ , the Bohr radius of the would-be toponium ground state,

$$r_Y/r_B = \left(\frac{4}{3}\alpha_s \frac{M_t}{2}\right)/M_H \approx 1/6, \quad (2)$$

the simple multiplicative treatment advocated above is sufficient for the presently required level of precision.

As discussed above, the impact on the total cross section from the variation of  $M_H$  is relatively small, less than one percent, both for the Tevatron and the LHC. Differential distributions, however, are significantly more sensitive to the Yukawa coupling. This is demonstrated in Figs. 14, 15, where the correction factors for the distribution with respect to  $M_{t\bar{t}}$  are evaluated for the Tevatron, LHC8 and LHC14 in the region close to threshold.

As expected from the previous discussion, differences around 5% between the cases  $M_H = 126$  GeV and 1 TeV are visible. It remains to be seen, whether the experimental mass resolution and normalization of the cross section will be sufficiently precise to pin down the 5%-effect and thus determine directly the Yukawa coupling  $g_Y$ . At the same time this approach requires a detailed theoretical understanding of the QCD predictions for the threshold behaviour, governed by the remnants of the bound states, as discussed in [42]. However, in any case this approach should allow to provide an upper limit on modifications of  $g_Y$  that might be postulated in theories beyond the Standard Model. Let us assume, for example, the case of an enhanced Yukawa coupling  $g_Y = 2g_Y^{SM}$ . This magnifies the Yukawa correction by a factor four and implies an enhancement of the cross section close to threshold by about 20%. (See dashed curves in Figs. 14, 15. Such an energy dependent offset relative to the SM prediction

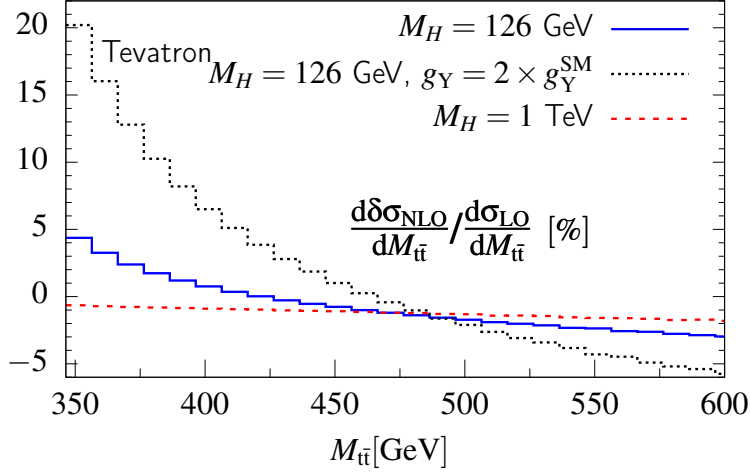


Figure 15: Same as Fig.14 but for the Tevatron.

should be visible in Tevatron or LHC analyses.

## 4 Outlook and conclusions

A sizable data sample has been collected by LHC experiments at a center-of-mass energy of 8 TeV, and the Higgs boson has been discovered with a mass of about 126 GeV. In view of these developments an update of the weak corrections to top quark pair production has been presented. We demonstrate that these corrections start to become important already for the 8 TeV run, if an experimental precision of 5 percent can be reached. This observation applies both for large transverse momenta, say above 500 GeV, where negative corrections around 5% are observed, and for top quark production close to threshold which is enhanced by about 5% due to the attractive Yukawa interaction. A detailed study of the top-antitop spectrum close to threshold could, therefore, determine the strength of the Yukawa coupling or, at least provide interesting upper limits. We also investigate the distribution of top and antitop with respect to their rapidity difference  $\Delta y_{t\bar{t}}$  for the subsample with large invariant mass and observe marked distortions of order 8% (LHC8) and 12% (LHC14). Clearly these effects might be misinterpreted as evidence for anomalous couplings and thus have to be well under control. Last not least we indicate a possible approach for combining QCD and weak corrections in the framework of a Monte Carlo generator.

### Acknowledgments

The work of J.H.K. was supported by BMBF Project 05H12VKE. Discussions with Jeannine Wagner-Kuhr on experimental issues are gratefully acknowledged. The work of A.S. has been

partly supported by the German Ministry of Education and Research (BMBF) under contract no. 05H12WWE.

## References

- [1] T. Aaltonen *et al.* [CDF and D0 Collaborations], Phys. Rev. D **86** (2012) 092003 [arXiv:1207.1069 [hep-ex]].
- [2] Tevatron electroweak working group, D0 Note 6363,
- [3] S. Moch and P. Uwer, Phys. Rev. D **78** (2008) 034003 [arXiv:0804.1476 [hep-ph]].
- [4] M. Aliev, H. Lacker, U. Langenfeld, S. Moch, P. Uwer and M. Wiedermann, Comput. Phys. Commun. **182** (2011) 1034 [arXiv:1007.1327 [hep-ph]].
- [5] S. Moch, P. Uwer and A. Vogt, Phys. Lett. B **714** (2012) 48 [arXiv:1203.6282 [hep-ph]].
- [6] M. Cacciari, M. Czakon, M. Mangano, A. Mitov and P. Nason, Phys. Lett. B **710** (2012) 612 [arXiv:1111.5869 [hep-ph]].
- [7] P. Baernreuther, M. Czakon and A. Mitov, Phys. Rev. Lett. **109** (2012) 132001 [arXiv:1204.5201 [hep-ph]].
- [8] M. Czakon and A. Mitov, JHEP **1212** (2012) 054 [arXiv:1207.0236 [hep-ph]].
- [9] M. Czakon and A. Mitov, JHEP **1301** (2013) 080 [arXiv:1210.6832 [hep-ph]].
- [10] M. Czakon, P. Fiedler and A. Mitov, arXiv:1303.6254 [hep-ph].
- [11] V. Ahrens, A. Ferroglia, M. Neubert, B. D. Pecjak and L. L. Yang, Phys. Lett. B **703** (2011) 135 [arXiv:1105.5824 [hep-ph]].
- [12] N. Kidonakis and B. D. Pecjak, Eur. Phys. J. C **72** (2012) 2084 [arXiv:1108.6063 [hep-ph]].
- [13] N. Kidonakis and R. Vogt, Phys. Rev. D **78** (2008) 074005 [arXiv:0805.3844 [hep-ph]].
- [14] M. Beneke, P. Falgari, S. Klein, J. Piclum, C. Schwinn, M. Ubiali and F. Yan, JHEP **1207** (2012) 194 [arXiv:1206.2454 [hep-ph]].
- [15] G. Aad *et al.* [ATLAS Collaboration], arXiv:1211.2202 [hep-ex].
- [16] S. Chatrchyan *et al.* [CMS Collaboration], arXiv:1211.3338 [hep-ex].
- [17] V. M. Abazov *et al.* [D0 Collaboration], arXiv:1207.0364 [hep-ex].
- [18] V. M. Abazov *et al.* [D0 Collaboration], Phys. Rev. D **84** (2011) 112005 [arXiv:1107.4995 [hep-ex]].
- [19] T. Aaltonen *et al.* [CDF Collaboration], arXiv:1211.1003 [hep-ex].

- [20] T. Aaltonen *et al.* [CDF Collaboration], Phys. Rev. D **83** (2011) 112003 [arXiv:1101.0034 [hep-ex]].
- [21] J. H. Kühn and G. Rodrigo, Phys. Rev. Lett. **81** (1998) 49 [hep-ph/9802268].
- [22] J. H. Kühn and G. Rodrigo, Phys. Rev. D **59** (1999) 054017 [hep-ph/9807420].
- [23] L. G. Almeida, G. F. Sterman and W. Vogelsang, Phys. Rev. D **78** (2008) 014008 [arXiv:0805.1885 [hep-ph]].
- [24] V. Ahrens, A. Ferroglia, M. Neubert, B. D. Pecjak and L. L. Yang, Phys. Rev. D **84** (2011) 074004 [arXiv:1106.6051 [hep-ph]].
- [25] W. Hollik and D. Pagani, Phys. Rev. D **84** (2011) 093003 [arXiv:1107.2606 [hep-ph]].
- [26] J. H. Kühn and G. Rodrigo, JHEP **1201** (2012) 063 [arXiv:1109.6830 [hep-ph]].
- [27] W. Bernreuther and Z. -G. Si, Phys. Rev. D **86** (2012) 034026 [arXiv:1205.6580 [hep-ph]].
- [28] [ATLAS Collaboration], ATLAS-CONF-2012-095.
- [29] W. Beenakker, A. Denner, W. Hollik, R. Mertig, T. Sack and D. Wackerroth, Nucl. Phys. B **411** (1994) 343.
- [30] J. H. Kühn, A. Scharf and P. Uwer, Eur. Phys. J. C **45** (2006) 139 [hep-ph/0508092].
- [31] W. Bernreuther, M. Fuecker and Z. G. Si, Phys. Lett. B **633** (2006) 54 [hep-ph/0508091].
- [32] W. Bernreuther, M. Fuecker and Z. -G. Si, Phys. Rev. D **74** (2006) 113005 [hep-ph/0610334].
- [33] J. H. Kühn, A. Scharf and P. Uwer, Eur. Phys. J. C **51** (2007) 37 [hep-ph/0610335].
- [34] S. Moretti, M. R. Nolten and D. A. Ross, Phys. Lett. B **639** (2006) 513 [Erratum-ibid. B **660** (2008) 607] [hep-ph/0603083].
- [35] W. Hollik and M. Kollar, Phys. Rev. D **77** (2008) 014008 [arXiv:0708.1697 [hep-ph]].
- [36] A. D. Martin, W. J. Stirling, R. S. Thorne and G. Watt, Eur. Phys. J. C **63** (2009) 189 [arXiv:0901.0002 [hep-ph]].
- [37] S. Kretzer, H. L. Lai, F. I. Olness and W. K. Tung, Phys. Rev. D **69** (2004) 114005 [hep-ph/0307022].
- [38] J. H. Kühn, A. A. Penin and V. A. Smirnov, Eur. Phys. J. C **17** (2000) 97 [hep-ph/9912503].
- [39] J. H. Kühn, S. Moch, A. A. Penin and V. A. Smirnov, Nucl. Phys. B **616** (2001) 286 [Erratum-ibid. B **648** (2003) 455] [hep-ph/0106298].
- [40] G. Aad *et al.* [ATLAS Collaboration], Phys. Lett. B **716** (2012) 1 [arXiv:1207.7214

[hep-ex]].

- [41] S. Chatrchyan *et al.* [CMS Collaboration], Phys. Lett. B **716** (2012) 30 [arXiv:1207.7235 [hep-ex]].
- [42] Y. Kiyo, J. H. Kühn, S. Moch, M. Steinhauser and P. Uwer, Eur. Phys. J. C **60** (2009) 375 [arXiv:0812.0919 [hep-ph]].
- [43] B. Grzadkowski, J. H. Kühn, P. Krawczyk and R. G. Stuart, Nucl. Phys. B **281** (1987) 18.
- [44] M. J. Strassler and M. E. Peskin, Phys. Rev. D **43** (1991) 1500.
- [45] V. S. Fadin and O. I. Yakovlev, Sov. J. Nucl. Phys. **53** (1991) 1053 [Yad. Fiz. **53** (1991) 1721].
- [46] M. Jezabek and J. H. Kühn, Phys. Lett. B **316** (1993) 360.
- [47] R. Harlander, M. Jezabek and J. H. Kühn, Acta Phys. Polon. B **27** (1996) 1781 [hep-ph/9506292].